Design of cold-formed stainless steel circular hollow section columns using direct strength method

Design of cold-formed stainless steel circular hollow section columns using direct strength method

Yuner Huang[1*] and Ben Young[2]

[1] *Institute for Infrastructure & Environment, School of Engineering, University of Edinburgh, United Kingdom*

[2] *Department of Civil Engineering, The University of Hong Kong, Pokfulam Road, Hong Kong*

ABSTRACT Cold-formed stainless steel circular hollow section (CHS) columns have been increasingly used in construction, due to its aesthetic appearance, long life-span and good ductility. It is shown that direct strength method (DSM) is capable of predicting cold-formed steel column strengths accurately. However, the DSM is developed for cold-formed steel sections with plate rather than curved elements, and thus its applicability for cold-formed stainless steel CHS is worth investigating. This paper presents a numerical investigation of cold-formed stainless steel CHS columns. A non-linear finite element model was developed and verified against column tests. Extensive parametric study of cold-formed duplex, lean duplex and ferritic stainless steel CHS columns has been performed to obtain column strengths. A total of 273 experimental and numerical cold-formed stainless steel CHS column strengths, which are obtained from previous researches and parametric study obtained from this study, are compared with the design strengths predicted by the current DSM. Reliability analysis was performed to evaluate the reliability of the design rules. It is shown that the current DSM provides unconservative and not reliable prediction for cold-formed stainless steel CHS columns. Therefore, modified DSM is proposed for cold-formed stainless steel CHS columns. It is shown that the modified design rule is more accurate than the current DSM, and the modified design rule is considered to be reliable.

Keywords: Circular hollow section; Cold-formed; Column; Direct strength method; Stainless steel; Structural design.

[*] Corresponding author. Tel.: +44 (0) 131-650-5739; fax: +44 (0) 131-650-6554.
E-mail address: Yuner.huang@ed.ac.uk.

1. Introduction

Cold-formed stainless steel has many advantages in construction applications, such as ease to construct, shiny appearance, long life span, relatively low maintenance cost, and better ductility compared with carbon steel. Therefore, it has been increasingly used in construction projects. Specifications [1, 2, 3] have been developed to facilitate engineers in designing stainless steel structural members. A wide range of experimental and numerical investigation on cold-formed stainless steel circular hollow section (CHS) columns has been conducted by previous researchers, including Young and Hartono [4], Ellobody and Young [5], Young and Ellobody [6], Talja [7], Gardner and Nethercot [8], Rasmussen and Hancock [9], and Bardi and Kyriakides [10]. Various types of austenitic and duplex stainless steel materials have been covered in previous investigation. Details of the previous experimental and numerical analysis are presented in Section 2.1 of this paper. The existing design rules, including American Specification [1], Australian/New Zealand Standard [2], European Code [3] as well as design rules proposed by Rasmussen and Hancock [9] and Rasmussen and Rondal [11], have been examined for designing stainless steel CHS section columns.

However, the direct strength method (DSM) proposed by Schafer and Pekoz [12] has not been examined for cold-formed stainless steel circular hollow section columns in previous research. The direct strength method has shown to be able to accurately predict compressive strengths of cold-formed steel columns, and it has been adopted by the North American Specification (AISI) [13, 14] for cold-formed steel structures. Direct strength method predicts the design strengths by calculating the nominal strengths of compressive members subjected to flexural, local and distortional buckling, and then takes the minimum value of these nominal strengths as the design strength. Full cross-sectional area, instead of effective area, is used in the direct strength method.

Thus, the calculation procedure of direct strength method is relatively convenient compared with the traditional effective method. It should be noted that the current direct strength method in AISI [13, 14] does not covers circular hollow section or stainless steel material. Zhu and Young [15] performed experimental and numerical analysis on aluminium circular hollow section columns, and compared the test and numerical results with design values calculated by the current direct strength method in AISI [13, 14]. It is shown that the current direct strength method generally provides conservative prediction for the aluminum non-welded columns of circular hollow sections. Design equation is proposed for aluminum alloy circular hollow section columns with transverse welds at the ends of the columns. Becque et al. [16] and Huang and Young [17] examined the direct strength method [13, 14] for designing stainless steel columns, and the modified direct strength method was proposed. However, the specimens in experimental and numerical program [16, 17] are rectangular and square hollow sections, but not circular hollow section. Therefore, there is a lack of investigation to examine the suitability of direct strength method for stainless steel circular hollow section columns.

The purpose of this paper is firstly to investigate the behaviour of stainless steel circular hollow section columns by performing extensive parametric study using finite element analysis (FEA). The finite element model (FEM) is verified with the available test results. Secondly, the suitability of current DSM for stainless steel circular hollow section column is assessed by comparing the numerical strength with design strength. Thirdly, design rules for stainless steel circular hollow section columns are proposed based on the current DSM. Lastly, reliability analysis was performed to assess the reliability of these design rules.

2. Summary of available data

Extensive experimental and numerical investigation on stainless steel circular hollow section column has been performed by previous researchers. A total of 165 available experimental and numerical data of stainless steel circular hollow section columns are used in this study, as summarized in Table 1. The data pool covers four different types of austenitic stainless steel and two types of duplex stainless steel, as shown in Table 1. The type 304 austenitic stainless steel circular hollow section columns have been investigated by Young and Hartono [4], Ellobody and Young [5], Young and Ellobody [6] and Gardner and Nethercot [8]. The available type 304 austenitic stainless steel circular hollow section column specimens ranged from stocky to slender sections with slenderness (D/t) of 5 to 200, where D and t are diameter and thickness of section. Tests on other types of austenitic stainless steel (316L and 304L) were conducted by Talja [7] and Rasmussen and Hancock [9], respectively. The slenderness of these specimens ranged from 34 – 48.6. Finite element analysis was performed for duplex stainless steel (EN 1.4462). The sections of these specimens ranged from stocky to slender, with D/t of 5 – 62.5. Experimental analysis of duplex stainless steel (EN 1.4410) was performed on sections with D/t ranging from 22.9 – 54.7.

The relationship of P_u/P_{ne} and λ_l for the available data is shown in Figure 1, where P_u is the experimental and numerical column strength, P_{ne} is the nominal member capacity and λ_l is the non-dimensional slenderness, as specified in the North American Specification [13]. It is shown that the slenderness of stainless steel CHS columns in previous researchers are smaller than 0.776 ($\lambda_l < 0.776$), while those with slenderness larger than 0.776 ($\lambda_l \geq 0.776$) are not available. It should be noted that the direct strength method predicts the column strength by considering the nominal member capacity for flexural buckling (P_{ne}) with $\lambda_l < 0.776$ and nominal member capacity for local buckling (P_{nl}) with $\lambda_l \geq 0.776$, and then take the minimum of P_{ne} and P_{nl} as the design strength.

Therefore, the lacking of experimental and numerical data of stainless steel CHS columns with slenderness larger than 0.776 leads to difficulties in assessing the suitability of current DSM for stainless steel CHS columns. Therefore, the parametric study in this paper focuses on the columns with slenderness larger than 0.776, which is detailed in Section 3 of this paper. The relationship of P_u/P_y and λ_c for the available data is shown in Figure 2, where P_y equals to yield stress of the material multiply by cross-sectional area, and λ_c is the non-dimensional slenderness to determine P_{ne}.

3. Finite element model

3.1 General

A non-linear finite element model (FEM) has been developed using the program ABAQUS version 6.11 [18]. The buckling behaviour of 15 cold-formed stainless steel circular hollow section (CHS) columns conducted by Young and Hartono [4] was simulated with the FEM. The measured geometry, material properties, initial local and overall geometric imperfections of the test specimens were used in the finite element model (FEM). Young and Ellobody [6] has pointed out that the effect of residual stresses on cold-formed stainless steel circular hollow section columns is negligible. Therefore, residual stresses are not included in the FEM.

3.2 Type of element and material modelling

A four-noded shell element with reduced integration S4R was used to model the CHS columns. A mesh size of 10 mm × 10 mm (length by width) was adopted. The measured stress-strain curves of each CHS were included in the model. Multi-linear stress-strain curves were used, including the

elastic part up to the proportional limit and the plastic curves of true stress and logarithmic true plastic strain. The measured Young's modulus reported in Young and Hartono [4] and Poisson's ratio of 0.3 are adopted in modelling the elastic part. The true plastic stress-strain curves calculated using Eqs. (1) and (2) were used in modelling the material properties of the columns, where σ, ε and E_o are the measured stress, strain and Young's modulus obtained from tensile coupon tests, and σ_{true} and $\varepsilon_{true,pl}$ are the true stress and true plastic strain, respectively.

$$\sigma_{true} = \sigma(1+\varepsilon) \tag{1}$$

$$\varepsilon_{true,pl} = \ln(1+\varepsilon) - \sigma_{true}/E_o \tag{2}$$

3.3 Boundary conditions and load applications

The test specimens [4] were compressed between fixed ends. According to the test procedures reported in Young and Hartono [4], the ends of the columns were simulated by restraining against all degrees of freedom, except for the displacement at the loaded end in the direction of the applied load. The nodes other than the two ends were free to translate and rotate in any directions. The boundary conditions were modelled by two reference points located at the centroids of two the ends, which are coupled with the surfaces of the cross-section at both ends. The axial loads were applied by specifying an axial displacement to the nodes at one end of the columns, which is identical to the column tests. The loading was applied by a static RIKS step. The nonlinear geometric parameter (*NLGEOM) was used to deal with the large displacement analysis.

3.4 Initial local and overall geometric imperfections

The measured local and overall geometric imperfections of the columns [4] were also included in the FEM. Initial local and overall geometric imperfections for the test specimens were measured

by Young & Ellobody [6] and Young & Hartono [4], respectively. The local and overall buckling modes were superposed on the column model. The BUCKLE procedure available in the ABAQUS library with the load applied within the step was used. The local buckling mode is obtained by carrying out Eigenvalue analysis using the first buckling mode (Eigenmode 1) using the measured specimen dimension. The overall buckling mode can be obtained by increasing the specimen thickness to obtain a small depth-to-thickness (D/t) ratio, and then carry out Eigenvalue analysis using the first buckling mode (Eigenmode 1). The values obtained from the first buckling mode predicted by the ABAQUS Eigenvalue analysis were normalized to 1.0, thus, the buckling mode was then factored by the measured magnitudes of the initial local and overall geometric imperfections of each column.

3.5 Validation of finite element model

The finite element model was validated with the CHS column tests conducted by Young and Hartono [4]. The results of the FEA were compared with the test strengths, as shown in Table 2. The mean value of experimental-to-numerical ultimate strength (P_{exp}/P_{FEA}) and axial shortening at ultimate strength (e_{exp}/e_{FEA}) ratio are 0.93 and 1.14, respectively, with the corresponding coefficient of variation (COV) of 0.021 and 0.146. The failure modes observed at ultimate load of the experimental specimens that involved material yielding (Y), local buckling (L), flexural buckling (F) and interaction of local and overall flexural buckling (L+F), are identical to those failure modes predicted from the FEA. Figure 3(a) shows the flexural buckling failure of specimen C2L2000, while Figure 3(b) shows the local buckling failure of specimen C3L3000.

4. Parametric study

Finite element analysis on 108 stainless steel CHS columns was carried out using the validated FEM. The parametric study includes cold-formed duplex (EN 1.4462) stainless steel, cold-formed lean duplex (EN 1.4162) stainless steel and cold-formed ferritic (EN 1.4003) stainless steel with 36 specimens for each material. The material properties of cold-formed duplex, lean duplex and ferritic stainless steel are obtained by Young & Lui [19], Huang & Young [20], and Huang & Young [21], respectively. The Young's modulus (E_o), 0.2 proof stress (yield strength) ($\sigma_{0.2}$), ultimate strength (σ_u) and Ramberg-Osgood parameter (n) used in the FEM for the three materials are summarized in Table 3.

The parametric study focus on specimens with slenderness (λ_l) greater than 0.776, as mentioned in Section 2.1 of this paper. Extensive range of cross-section and column slenderness is designed for the parametric study, including 12 CHS with 3 different effective lengths in each section for each material. The diameter-to-thickness (D/t) of the 12 sections varies from 100 to 400, where D is the diameter and t is the thickness of the section. The effective length (l_e) of the fixed-ended column in the parametric study is equal to half of the specimen length, with the effective length factor (k) taken as 0.5. The non-dimensional slenderness (λ_l) to determine nominal member capacity for local buckling (P_{nl}) ranges from 0.44 to 1.34.

The average measured overall geometric imperfections for the experimental specimens reported in Young and Hartono [4] is $L/2559$. Thus, slightly conservative rounded numbers of $L/2500$ were used as the overall imperfections in the parametric study. Local imperfection of the test specimens were measured by Young & Ellobody [6], which is equal to 3.2% of the plate thickness of the specimens. Therefore, local imperfection equals to 3.2% of the plate thickness is

used in the parametric study. The column strength (P_{FEA}) and failure modes of the specimens in parametric study are summarized in Table 4.

The specimens are labelled such that the cross-section dimensions and the specimen length could be identified, as shown in Table 4. For example, the label "D100×1L1000" defines the following CHS column:

- The first letter indicates that the material is duplex stainless steel (D). The lean duplex stainless steel and ferritic stainless steel are represented by letters "L" and "F", respectively.
- The cross-section dimension (diameter × thickness) is followed by the first letter. The specimen diameter is 100 mm and thickness is 1 mm.
- The letter "L" after the dimension indicates the length of the specimen.
- The last four digits are the length of the specimen (1000 mm).

The reliability of the column design rules was evaluated using reliability analysis. Reliability analysis is detailed in the Commentary of the ASCE Specifications [1]. A target reliability index (β) of 2.5 for stainless steel structural members is used in this study. The design rules are considered to be reliable if the reliability index is greater than 2.5. The resistance factors (ϕ) of 0.85 for concentrically loaded compression members, as recommended by North American Specification (AISI) [13, 14], were used in the reliability analysis. The load combination of 1.2DL+1.6LL in AISI was used for reliability analysis. The Eq. 6.2-2 in the ASCE Specification was used in calculating the reliability index. The statistical parameters M_m = 1.10, F_m = 1.00, V_m = 0.10 and V_F = 0.05, which are the mean values and coefficients of variation for material properties and fabrication factors for flexural buckling members in the commentary of the ASCE Specification were adopted. The mean value (P_m) and coefficient of variation of tested-to-predicted load ratio (V_P) are shown in Table 5 for all specimens. In calculating the reliability index, the

correction factor Eq. K2.1.1-4 in the AISI [13] was used to account for the influence due to a small number of tests. Result of reliability analysis is shown in Table 5.

5. Comparison of experimental and numerical strengths with design strengths

The direct strength method in this study was based on the clauses E3.2.1 for compression members subjected to local buckling interacting with global buckling in AISI S100 [13]. The direct strength method is developed for sections with plate rather than curved elements. It should be noted that circular hollow section is not covered by the direct strength method (DSM). Therefore, the applicability of DSM for stainless steel CHS columns can be assessed using the available data and numerical data in parametric study. According to clause E3.2.1, the nominal axial strength for compressive members subjected to local buckling (P_{nl}) and global buckling (P_{ne}) shall be determined by Eqs (3) and (4). The column capacity calculated by direct strength method P_{DSM} is the lower value of P_{nl} and P_{ne}. It should be noted that distortional buckling does not occur in CHS columns. Calculation of the elastic local buckling load (P_{crl}) is required in determining the local buckling strength. The software Thin-Wall using a rational elastic finite strip buckling analysis [22] was used to determine the elastic local buckling stress (f_{ol}) by applying buckling analysis to each section of the specimens with the accuracy of 5 mm half-wave length. The signature curve and local buckling of CHS obtained from the finite strip analysis are shown in Figure 4.

$$P_{nl} = \begin{cases} P_{ne} & \text{for } \lambda_l < 0.776 \\ \left[1 - 0.15\left(\frac{P_{crl}}{P_{ne}}\right)^{0.4}\right]\left(\frac{P_{crl}}{P_{ne}}\right)^{0.4} P_{ne} & \text{for } \lambda_l \geq 0.776 \end{cases} \quad (3)$$

$$P_{ne} = \begin{cases} \left(0.658^{\lambda_c^2}\right)P_y & \text{for } \lambda_c < 1.5 \\ \left(\frac{0.877}{\lambda_c^2}\right)P_y & \text{for } \lambda_c \geq 1.5 \end{cases} \quad (4)$$

where λ_c is the non-dimensional slenderness to determine P_{ne}, P_y is the nominal yield capacity of the member in compression, P_{crl} is the elastic local buckling load = $f_{ol} \times A$, and A is the cross-sectional area of specimen.

The DSM to predict column strength is assessed by comparing the experimental and numerical column strengths with design strengths. The relationship of P_u/P_{ne} and λ_l for all specimens, including available data and parametric study, is shown in Figure 1. The relationship of P_u/P_y and λ_c for specimens with $\lambda_l \geq 0.776$ is shown in Figure 2. Comparison of experimental and numerical column strength with design strength is shown in Table 5. Generally speaking, the current DSM is unconservative in predicting the stainless steel CHS columns. For all specimens, the mean value of P_u / P_{DSM} ratio equals to 0.96, with the coefficient of variation (COV) equals to 0.130. The design rule is considered to be not reliable with the reliability index (β) equals to 2.36, which is smaller than the target value. For specimens with $\lambda_l < 0.776$ and $\lambda_l \geq 0.776$, the mean values of P_u / P_{DSM} ratio equal to 0.99 and 0.92, with the coefficient of variation (COV) equals to 0.138 and

0.090, respectively. Similarly, the reliability indices (β) of these two groups of specimens are smaller than the target value. Therefore, it is important to modify the current DSM, so that the DSM is able to provide accurate and reliable prediction for stainless steel CHS columns.

It is shown from Figures 1 and 2 that the current DSM general provides accurate prediction for the available data with slenderness $\lambda_l < 0.776$, while it is unconservative for specimens with slenderness $\lambda_l \geq 0.776$. Therefore, it is suggested that the coefficients in Eq. (4) does not need to change, except that the intersection point between P_{ne} and P_{nl} changes from 0.776 to 0.77. The Eq. (3) should be modified to provide a more accurate prediction. It is suggested that P_{ne} and P_{nl} to be calculated using Eqs (5) and (6) in the modified direct strength method, and the lower value of P_{ne} and P_{nl} is taken as the design strength (P^*_{DSM}) predicted by the modified DSM:

$$P_{nl} = \begin{cases} P_{ne} & \text{for } \lambda_l < 0.77 \\ \left[1 - 0.2\left(\frac{P_{crl}}{P_{ne}}\right)^{0.65}\right]\left(\frac{P_{crl}}{P_{ne}}\right)^{0.65} P_{ne} & \text{for } \lambda_l \geq 0.77 \end{cases} \quad (5)$$

$$P_{ne} = \begin{cases} \left(0.658^{\lambda_c^2}\right) P_y & \text{for } \lambda_c < 1.5 \\ \left(\frac{0.877}{\lambda_c^2}\right) P_y & \text{for } \lambda_c \geq 1.5 \end{cases} \quad (6)$$

The design strength predicted by the modified DSM is represented by P^*_{DSM}. The comparison results of experimental and numerical column strengths (P_u) over design strength (P^*_{DSM}) were shown in Table 5 and Figures 1 and 2. It is shown that the modified DSM provides a more accurate

and less scattered prediction for stainless steel CHS columns. The mean values of P_u / P^*_{DSM} ratio equals to 0.99, 0.99 and 1.00, with COV of 0.121, 0.139, and 0.079 for all specimens, specimens with slenderness $\lambda_l < 0.77$, and specimens with slenderness $\lambda_l \geq 0.77$, respectively. The revised DSM method is considered to be reliable for all specimens, with the reliability index (β) equals to the target value of 2.50. Comparison of experimental and numerical column strengths with the design strengths calculated by modified DSM is shown in Figure 1.

6. Conclusions

An investigation on the design of cold-formed stainless steel circular hollow section columns using direct strength method is presented in this paper. A total of 165 available experimental and numerical cold-formed stainless steel circular hollow section column strengths by previous researchers were collected. A finite element model was developed and compared with experimental results reported by Young and Hartono [4]. Good agreement between the finite element and experimental results was observed. A wide range of parametric study with 108 cold-formed stainless steel circular hollow section columns was conducted using the verified finite element model. The parametric study includes cold-formed duplex, lean duplex and ferritic stainless steel. The column strengths obtained from the parametric study, together with the available data of stainless steel circular hollow section columns, were compared with the design strengths calculated by the current direct strength method in North American Specification (AISI) [13].

It is shown that the current direct strength method provides unconservative and scattered prediction to the specimens investigated in this study, especially to the slender sections with slenderness λ_l greater than 0.776, due to the fact that the previous researches do not cover the range

of λ_l greater than 0.776 for cold-formed stainless steel circular hollow section columns. A modified direct strength method is proposed in this paper, to facilitate the design of cold-formed stainless steel circular hollow section columns. It is shown that the modified direct strength method provides more accurate and reliable predictions, especially for slender specimens with λ_l greater than 0.776.

Acknowledgement

The research work described in this paper was supported by a grant from The University of Hong Kong under the seed funding program for basic research.

Notation

The following symbols are used in this paper:

A = cross-sectional area;

D = diameter of specimen;

E_o = initial Young's modulus;

e_{exp} = axial displacement at ultimate load obtained from experimental program

e_{FEA} = axial displacement at ultimate load obtained from finite element analysis

F_m = mean value of fabrication factor;

f_{ol} = elastic local buckling stress;

k = effective length factor;

L = length of specimen;

l_e = effective length of specimen;

M_m = mean value of material factor;

n = Ramberg-Osgood parameter;

P_{crl} = elastic local buckling load;

P_{DSM} = design strengths calculated using direct strength method;

P_{exp} = column strength obtained from experimental program;

P_{FEA} = column strength obtained from finite element analysis;

P_{ne} = nominal member capacity of a member in compression for flexural buckling;

P_{nl} = nominal member capacity of a member in compression for local buckling;

P_u = compressive capacity of column members;

P_y = the nominal yield capacity of the member in compression;

P^*_{DSM} = design strengths calculated using modified direct strength method;

t = thickness of specimen;

V_F = coefficient of variation of fabrication factor;

V_m = coefficient of variation of material factor;

V_p = coefficient of variation of tested-to-predicted load ratio;

β = reliability index;

ε = tensile strain;

$\varepsilon_{true,pl}$ = plastic true strain;

ϕ = resistance factor;

λ_c = non-dimensional slenderness to determine P_{ne};

λ_l = non-dimensional slenderness to determine P_{nl};

σ = tensile stress or normal stress;

σ_{true} = true stress;

σ_u = static tensile strength;

$\sigma_{0.2}$ = static 0.2% tensile proof stress;

References

[1] ASCE. Specification for the design of cold-formed stainless steel structural members. SEI/ASCE 8-02; Reston, VA: American Society of Civil Engineers; 2002.

[2] AS/NZS. Cold-formed stainless steel structures. Australian/New Zealand Standard, AS/NZS 4673:2001. Sydney (Australia): Standards Australia; 2001.

[3] EC3. Design of steel structures – Part 1.4: General rules – Supplementary rules for stainless steels. European Committee for Standardization, ENV 1993-1-4, CEN, Brussels; 2006.

[4] Young B., Hartono W. "Compression tests of stainless steel tubular members" Journal of Structural Engineering, 2002, 128 (6): 754-761.

[5] Ellobody E., Young B. "Investigation of cold-formed stainless steel non-slender circular hollow section columns", *Steel and Composite Structures*, 2007, 7(4): 321-337.

[6] Young B., Ellobody E. "Column design of cold-formed stainless steel slender circular hollow sections", *Steel and Composite Structures*, 2006, 6 (4): 285-302.

[7] Talja A. Test report on welded I and CHS beams, columns and beams-columns. Report to ECSC. 1997. VTT Building Technology, Finland.

[8] Gardner L., Nethercot D.A. "Experiments on stainless steel hollow sections – Part 1: Material and cross-sectional behaviour", *Journal of Constructional Steel Research*, 2004, 60(9): 1291-1318.

[9] Rasmussen K.J.R., Hancock G.J. "Design of cold-formed stainless steel tubular members, I: Columns." *Journal of Structural Engineering ASCE*, 1993; 119(8):2349–67.

[10] Bardi F.C., Kyriakides S. "Plastic buckling of circular tubes under axial compression – Part I: Experiments". *International Journal of Mechanical Sciences*. 2006, 48(8): 830-841.

[11] Rasmussen, K. J. R., Rondal, J. ''Strength curves for metal columns.'' *Journal of Structural*

Engineering ASCE, 1997; 123(6), 721–728.

[12] Schafer B.W., Pekoz T. "Direct strength prediction of cold-formed steel members using numerical elastic buckling solutions". In: Proceeding of 14th international specialty conference on cold-formed steel structures. University of Missouri-Rolla, Rolla, MO, 1998. 69 – 76.

[13] AISI S100. North American Specification for the design of cold-formed steel structural members. AISI S100-16, North American Cold-formed Steel Specification, American Iron and Steel Institute, Washington, D.C.; 2016.

[14] AISI S100. Commentary on North American Specification for the design of cold- formed steel structural members. AISI S100-16-C, North American Cold-formed steel specification. American Iron and Steel Institute, Washington, D. C.; 2016.

[15] Zhu J.H., Young B. "Numerical investigation and design of aluminium alloy circular hollow section columns". *Thin-Walled Structures*, 2008; 46: 1437 – 1449.

[16] Becque J., Lecce M., Rasmussen K.J.R. "The direct strength method for stainless steel compression members". *Journal of Constructional Steel Research*, 2008; 64: 1231 – 1238.

[17] Huang Y., Young B. "Structural performance of cold-formed lean duplex stainless steel columns". *Thin-Walled Structures*, 2014; 83: 59 – 69.

[18] ABAQUS Standard User's Manual. Dassault Systemes Simulia Corp., Version 6.11, USA; 2011.

[19] Young B., Lui W.M. "Behavior of cold-formed high strength stainless steel sections". *Journal of Structural Engineering ASCE*, 2005; 131(11): 1738 - 1745.

[20] Huang Y., Young B. "Material properties of cold-formed lean duplex stainless steel sections". *Thin-Walled Structures*, 2012; 54: 72-81.

[21] Huang Y., Young B. “The art of coupon tests”. *Journal of Constructional Steel Research* , 2014; 96: 159-175.

[22] Papangelis J.P., Hancock G.J. “Computer analysis of thin-walled structural members”. *Computers and Structures*, 1995; 56(1):157 – 76.

Reference	Approach	Material	Type		# of data
			EN	ASTM	
Young & Hartono [4]	Tests	Austenitic	1.4301	304	16
Ellobody & Young [5]	FEA	Austenitic	1.4301	304	35
		Duplex	1.4462	S31803	35
Young & Ellobody [6]	FEA	Austenitic	1.4301	304	42
Talja [7]	Tests	Austenitic	1.4435	316L	5
			1.4541	321	4
Gardner & Nethercot [8]	Tests	Austenitic	1.4301	304	4
Rasmussen & Hancock [9]	Tests	Austenitic	1.4306	304L	6
Bardi & Kyriakides [10]	Tests	Duplex	1.4410	S32750	20
				Total	165

Table 1: Summary of available cold-formed stainless steel CHS column strengths

Specimen	Tests*			FEA			Comparison	
	P_{exp} (kN)	e_{exp} (mm)	Failure mode	P_{FEA} (kN)	e_{FEA} (mm)	Failure mode	$\frac{P_{exp}}{P_{FEA}}$	$\frac{e_{exp}}{e_{FEA}}$
C1L550	235.2	16.9	Y	247.9	12.9	Y	0.95	1.31
C1L1000	198.4	10.3	Y	213.3	9.3	Y	0.93	1.10
C1L1500	177.4	5.8	F	192.1	6.3	F	0.92	0.92
C1L2000	165.1	4.8	F	176.1	5.0	F	0.94	0.97
C1L2500	151.6	5.4	F	158.4	5.2	F	0.96	1.04
C1L3000	133.4	5.0	F	147.4	5.1	F	0.91	0.98
C2L550	495.6	9.41	Y	528.7	7.2	Y	0.94	1.31
C2L1000	474.9	14.64	L+F	499.1	10	L+F	0.95	1.46
C2L1500	461.0	15.92	L+F	487.2	11.9	L+F	0.95	1.34
C2L2000	431.6	13.32	F	463.4	12	F	0.93	1.11
C3L1000	1123.9	8.05	Y	1231.8	8.5	Y	0.91	0.95
C3L1500	1119.7	14.38	Y	1203.1	11.6	Y	0.93	1.24
C3L2000	1087.8	14.53	L	1170.03	13.48	L	0.93	1.07
C3L2500	1045.7	19.12	L	1073.9	15.85	L	0.97	1.21
C3L3000	1009.5	15.64	L	1123.9	15.01	L	0.90	1.04
						Mean	0.93	1.14
						COV	0.021	0.146

*The test results are reported in Young and Hartono [4]

Table 2: Comparison between test and finite element results

Material	E_o (GPa)	$\sigma_{0.2}$ (MPa)	σ_u (MPa)	n
Duplex (D) [19]	226	757	854	3
Lean duplex (L) [20]	202	664	788	4
Ferritic (F) [21]	205	459	464	7

Table 3: Material properties of stainless steel materials in parametric study

Specimen	P_{FEA} (kN)	Failure mode	f_{crl} (MPa)	λ_l	P_{DSM} (kN)
D100×1L1000	219.1	Y	1577.0	0.66	213.6
D100×1L3000	165.6	L	1577.0	0.59	170.2
D100×1L5000	90.3	L+F	1577.0	0.47	108.1
D150×1L1000	320.5	L	1050.0	0.82	316.7
D150×1L3000	292.3	L+F	1050.0	0.78	295.5
D150×1L5000	230.1	L+F	1050.0	0.70	241.8
D200×1L1000	374.6	L	786.9	0.94	387.1
D200×1L3000	368.5	L+F	786.9	0.92	372.7
D200×1L5000	365.9	L+F	786.9	0.87	345.3
D250×1L1000	442.0	L	629.2	1.06	450.7
D250×1L3000	431.6	L+F	629.2	1.04	440.0
D250×1L5000	416.3	L+F	629.2	1.00	419.4
D300×1L1000	495.0	L	524.1	1.16	509.5
D300×1L3000	471.9	L+F	524.1	1.15	501.1
D300×1L5000	465.8	L+F	524.1	1.12	484.9
D350×1L1000	531.1	L	449.2	1.25	564.5
D350×1L3000	517.9	L+F	449.2	1.24	557.8
D350×1L5000	511.5	L+F	449.2	1.22	544.5
D400×1L1000	557.6	L	393.0	1.34	616.6
D400×1L3000	536.3	L+F	393.0	1.33	611.0
D400×1L5000	529.1	L+F	393.0	1.31	599.9
D400×2L1000	1608.7	Y	786.9	0.95	1553.8
D400×2L3000	1586.5	L	786.9	0.94	1539.2
D400×2L5000	1566.7	L+F	786.9	0.93	1510.2
D500×2L1000	1717.6	L	629.2	1.06	1806.9
D500×2L3000	1709.4	L	629.2	1.05	1796.1
D500×2L5000	1696.0	L+F	629.2	1.05	1774.7
D600×2L1000	1898.4	L	524.1	1.16	2041.0
D600×2L3000	1650.3	L	524.1	1.16	2032.6
D600×2L5000	1600.4	L	524.1	1.15	2015.9
D700×2L1000	2066.9	L	449.2	1.25	2260.6
D700×2L3000	1754.3	L	449.2	1.25	2253.9
D700×2L5000	1675.5	L	449.2	1.25	2240.4
D800×2L1000	2161.3	L	393.0	1.34	2468.4
D800×2L3000	1932.3	L	393.0	1.34	2462.8
D800×2L5000	1923.1	L	393.0	1.33	2451.6
L100×1L1000	218.1	Y	1479.0	0.66	200.6
L100×1L3000	157.3	L	1479.0	0.59	159.8
L100×1L5000	89.0	L+F	1479.0	0.47	101.3
L150×1L1000	314.1	L	983.6	0.82	297.2

L150×1L3000	283.2	L+F	983.6	0.78	277.3
L150×1L5000	216.2	L+F	983.6	0.70	226.9
L200×1L1000	359.0	L	736.8	0.95	363.2
L200×1L3000	356.0	L+F	736.8	0.92	349.6
L200×1L5000	348.1	L+F	736.8	0.87	323.9
L250×1L1000	418.7	L	588.2	1.06	422.6
L250×1L3000	407.8	L+F	588.2	1.04	412.6
L250×1L5000	402.1	L+F	588.2	1.00	393.2
L300×1L1000	466.7	L	489.8	1.16	477.7
L300×1L3000	449.5	L+F	489.8	1.15	469.8
L300×1L5000	445.0	L+F	489.8	1.12	454.5
L350×1L1000	490.1	L	419.8	1.26	529.3
L350×1L3000	469.1	L+F	419.8	1.24	523.0
L350×1L5000	464.2	L+F	419.8	1.22	510.5
L400×1L1000	507.7	L	367.5	1.34	578.2
L400×1L3000	487.1	L+F	367.5	1.33	572.9
L400×1L5000	485.7	L+F	367.5	1.32	562.5
L400×2L1000	1558.8	Y	736.8	0.95	1457.9
L400×2L3000	1531.0	L	736.8	0.94	1444.1
L400×2L5000	1512.1	L+F	736.8	0.93	1416.8
L500×2L1000	1656.3	L	588.2	1.06	1694.4
L500×2L3000	1612.1	L	588.2	1.06	1684.2
L500×2L5000	1730.4	L+F	588.2	1.05	1664.1
L600×2L1000	1772.6	L	489.8	1.16	1913.6
L600×2L3000	1491.8	L	489.8	1.16	1905.8
L600×2L5000	1410.3	L	489.8	1.15	1890.1
L700×2L1000	1910.6	L	419.8	1.26	2119.6
L700×2L3000	1520.5	L	419.8	1.25	2113.2
L700×2L5000	1516.1	L	419.8	1.25	2100.5
L800×2L1000	1958.8	L	367.5	1.34	2314.8
L800×2L3000	1782.3	L	367.5	1.34	2309.5
L800×2L5000	1769.2	L	367.5	1.34	2299.0
F100×1L1000	137.6	Y	1510.0	0.56	147.1
F100×1L3000	116.6	L	1510.0	0.52	125.2
F100×1L5000	83.6	L+F	1510.0	0.44	90.6
F150×1L1000	204.0	L	1005.0	0.69	224.0
F150×1L3000	191.2	L+F	1005.0	0.67	208.5
F150×1L5000	168.3	L+F	1005.0	0.62	180.8
F200×1L1000	260.1	L	753.4	0.80	294.9
F200×1L3000	257.8	L+F	753.4	0.78	286.9

F200×1L5000	245.7	L+F	753.4	0.75	266.3
F250×1L1000	314.9	L	602.5	0.89	344.2
F250×1L3000	310.6	L+F	602.5	0.88	338.3
F250×1L5000	306.9	L+F	602.5	0.86	326.7
F300×1L1000	366.0	L	502.0	0.98	389.8
F300×1L3000	347.2	L+F	502.0	0.97	385.2
F300×1L5000	344.4	L+F	502.0	0.95	376.1
F350×1L1000	408.1	L	430.1	1.06	432.5
F350×1L3000	401.1	L+F	430.1	1.05	428.7
F350×1L5000	397.4	L+F	430.1	1.04	421.3
F400×1L1000	447.0	L	376.3	1.13	472.9
F400×1L3000	441.8	L+F	376.3	1.13	469.8
F400×1L5000	432.6	L+F	376.3	1.12	463.6
F400×2L1000	1081.7	Y	753.4	0.80	1182.7
F400×2L3000	1070.6	L	753.4	0.80	1174.6
F400×2L5000	1062.4	L+F	753.4	0.79	1158.6
F500×2L1000	1254.2	L	602.5	0.89	1379.0
F500×2L3000	1243.1	L	602.5	0.89	1373.1
F500×2L5000	1232.8	L+F	602.5	0.89	1361.2
F600×2L1000	1440.0	L	502.0	0.98	1560.9
F600×2L3000	1249.8	L	502.0	0.98	1556.3
F600×2L5000	1200.3	L	502.0	0.97	1547.0
F700×2L1000	1612.6	L	430.1	1.06	1731.3
F700×2L3000	1366.1	L	430.1	1.06	1727.5
F700×2L5000	1353.4	L	430.1	1.05	1720.1
F800×2L1000	1748.0	L	376.3	1.13	1892.8
F800×2L3000	1566.0	L	376.3	1.13	1889.6
F800×2L5000	1546.0	L	376.3	1.13	1883.4

Table 4: Summary of finite element results in parametric study

	P_u / P_{DSM}			P_u / P^*_{DSM}		
	All	$\lambda_l < 0.776$	$\lambda_l \geq 0.776$	All	$\lambda_l < 0.77$	$\lambda_l \geq 0.77$
# of data	273	181	92	273	180	93
Mean (P_m)	0.96	0.99	0.92	0.99	0.99	1.00
COV (V_p)	0.130	0.138	0.090	0.121	0.139	0.079
Resistance factor (ϕ)	0.85	0.85	0.85	0.85	0.85	0.85
Reliability index (β)	2.36	2.42	2.34	2.50	2.41	2.69

Table 5: Comparison of test and FEA results with design strengths

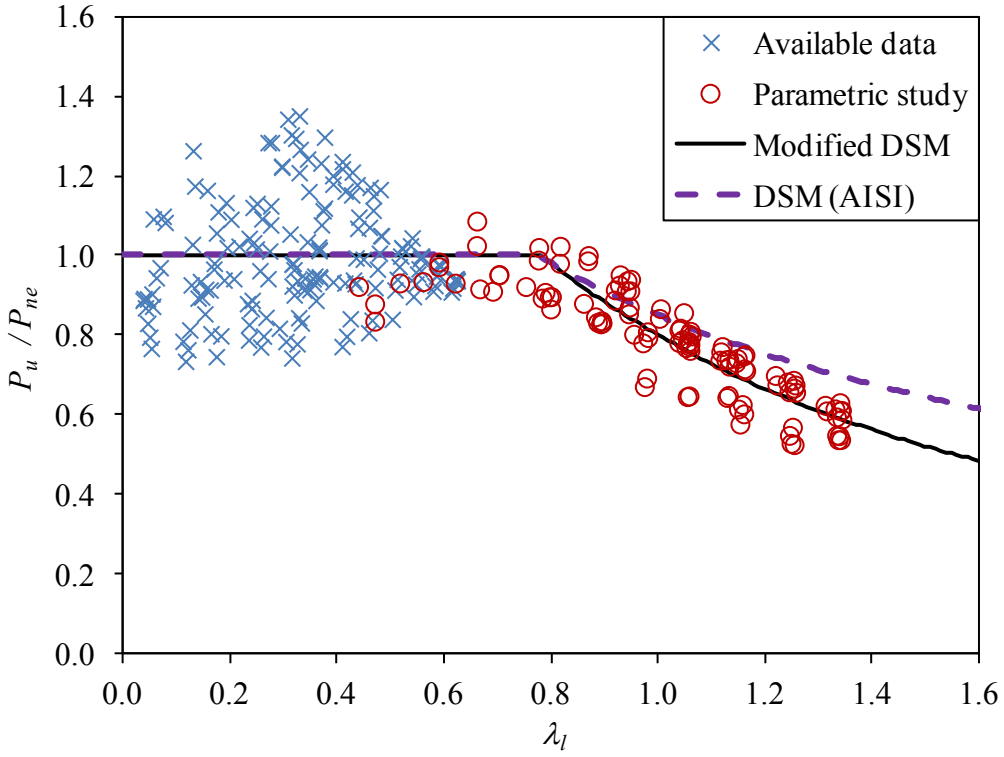

Figure 1: Comparison of tests and numerical results with design strengths by DSM

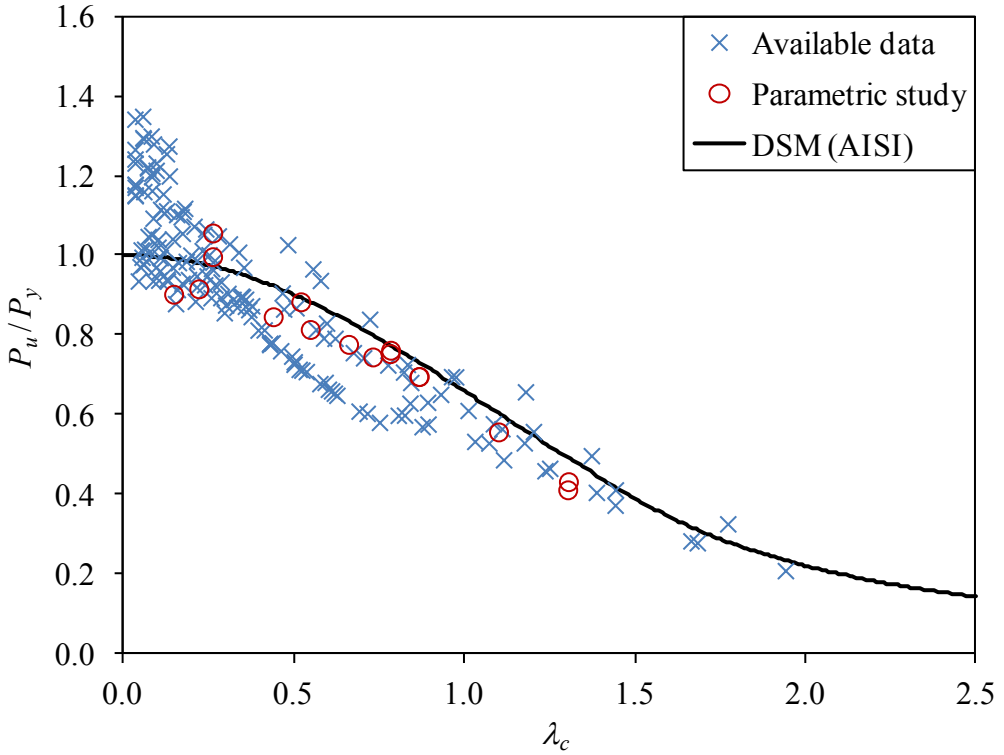

Figure 2: Comparison of tests and numerical results with design strengths by DSM

(a) (b)

Figure 3: Finite element model of (a) specimen C2L2000 failed by flexural buckling, and (b) specimen C3L3000 failed by local buckling

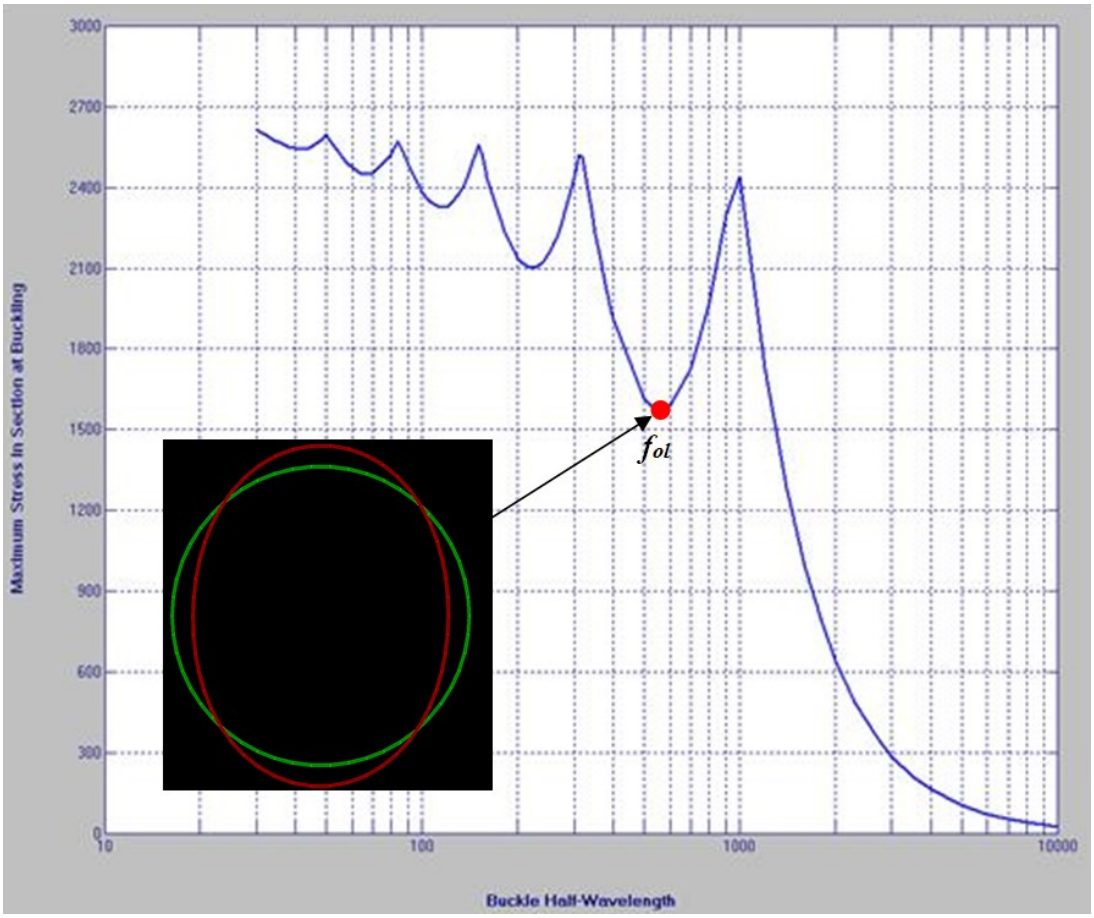

Figure 4: A typical signature curve obtained from thin-wall program (Ref. [22])